PCCP

PAPER

Received 00th January 20xx,
Accepted 00th January 20xx
DOI: 10.1039/x0xx00000x

www.rsc.org/

Photoinduced Hole Transfer in QD-Phthalocyanine Hybrids

M. Arvani,*[a] K. Virkki,[b] F. Abou-Chahine,[b] A. Efimov,[b] N. V. Tkachenko*[b] and D. Lupo*[a]

A series of CdSe quantum dot (QD) – phthalocyanine (Pc) hybrids were synthesized and their photophysics were studied by steady state and time-resolved spectroscopic methods. Emission of QD was progressively quenched upon increasing concentration of Pc in the hybrids. A detailed transient absorption study of the hybrids revealed that the mechanism of the quenching is charge separation, resulting in formation of hybrids with negatively charged QD and Pc cation. Direct photo-excitation of Pc did not show any detectable interaction between the excited state of Pc and the QD to which it is attached. An explanation is proposed, based on the suggestion that the energy of the Pc lowest unoccupied molecular orbital (LUMO) is lower than the lower edge of the QD conduction band, while the energy of the Pc highest occupied molecular orbital (HOMO) is sufficiently higher than the high energy edge of the QD valence band (VB), thus permitting hole transfer from the QD VB to the Pc HOMO after photo-excitation of QD.

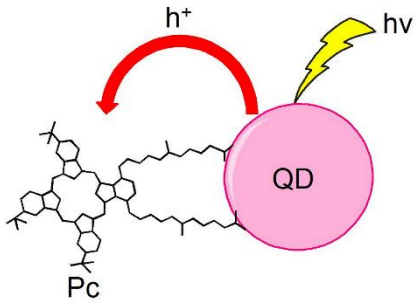

1 Introduction

Semiconductor quantum dot (QD) – organic dye hybrids attract significant interest from researchers as new design paradigms for advanced photoactive nanosystems, which can combine benefits of both components in a single architecture.[1–3] An advantage of a semiconductor QD is relative ease of tailoring the optical properties by changing its size[4,5] whereas organic dyes can be crafted with various peripheral groups to permit supramolecular design and thus simplify the development of complex hybrid nanostructures.[6–8] Photophysical studies of such hybrids are not numerous but the number of publications is growing rapidly, since this knowledge is crucial for applications of such hybrids in nanophotonics and optoelectronics.[9–12] Two types of photoinduced interactions are energy and charge transfer, and there are a few examples when competition between these two reactions was observed.[13–15] Photoinduced charge separation is the most common objective in developing new hybrids because of prospects of hybrid applications in solar cell devices.[16–18]

[a] Department of Electronics and Communications Engineering, Tampere University of Technology, 33720 Tampere, Finland. E-mail: maedeh.Arvani@tut.fi and Donald.Lupo@tut.fi
[b] Department of Chemistry and Bioengineering, Tampere University of Technology, 33720 Tampere, Finland. E-mail: Nikolai.Tkachenko@tut.fi

† *Electronic Supplementary Information (ESI) available: [procedures of synthesis of phthalocyanine, DPV measurements, absorption and emission spectra, dependence of Pc absorbance ratio at 720 and 635 nm on relative concentration of Pc, emission decays and emission lifetime quenching, transient absorption measurements of QDs and QD-Pc hybrids not shown in the main text]. See DOI: 10.1039/x0xx00000x*

CdSe QDs are probably the most well developed and studied quantum dots. The energy of the conduction band (CB) of CdSe QDs is well matched to that of lowest unoccupied molecular orbital (LUMO) of typical organic electron donating molecules, and CdSe QDs were found to act as electron donors in conjunction with typical electron acceptors such as fullerene C_{60}[19–21] and viologen.[22] These studies have motivated theoretical and computational modeling of the photoinduced electron transfer from QDs to organic dyes adsorbed on its surface.[23,24] At the same time, reports of photoinduced electron transfer from organic dye to QD are few, although the estimated low edge of the conduction band of CdSe QD is lower than the LUMO of some organic electron donors. Electron transfer to CdSe QD was reported for QD hybrids with rhodamine B,[13] porphyrin drivatives[25] and for CdS and bithiophene hybrids.[26] However, there are many other classes of organic compounds with good electron donating properties that are used in numerous designs of organic donor-acceptor systems. One class of such compounds is phthalocyanine derivatives,[27,28] which has not been exploited yet. The interest in this research is motivated by the possibility to achieve photoinduced electron transfer in both directions, from QD and to QD, which promises to open a new range of applications.

In this study we report evidence for a hole transfer from a QD to Pc in QD-Pc hybrids as a path to directing charge transfer between QDs and photo-ligands, based on an extensive study of the time-resolved photophysics of a range of QD-Pc hybrids. Surprisingly, the electronic interaction between QD and Pc is only observed when the QD is optically excited, not when the Pc is excited directly.

2 Methods and materials

QDs of five different sizes were purchased from Strem Chemicals, Inc. and their properties are summarized in Table 1.

The phthalocyanine (Scheme 1) used in this study was produced from a corresponding dipropanol derivative as presented in the Supporting Information (SI). The carboxylic acid functionalized Pc derivative is used instead of the more widely used thiol derivative because thiols were found to have a quenching effect on the QD emission, whereas the carboxylic acid group has almost no quenching effect but provides reasonably good binding to QDs. Another advantage of the carboxyl linker over the thiol is a simpler synthesis of the compounds. All measurements were performed at room temperature.

Differential pulse voltammetry (DPV) measurements for the estimation of energy levels were performed using a platinum working electrode, a Ag/AgCl reference electrode and a graphite rod counter electrode.[29] Ferrocene was added as an internal reference, and all the potentials were referenced to the Fc/Fc^+. DPV measurements were performed from −2.0 to +2.0 V. The supporting electrolyte was 0.1 M tetrabutylammonium hexafluorophosphate ($TBAPF_6$) in $CHCl_3$. The pulse time was 20 ms, and the pulse amplitude was 20 mV. Before each run, the surface of the working electrode was polished with an aluminum suspension.

Absorption spectra were measured using a Shimadzu UV-3600 spectrophotometer and fluorescence spectra were measured with an ISA-Jobin Yvon-SPEX-Horiba Fluorolog-2-111 fluorometer and

Table 1 QD sizes, absorption (λ_{abs}) and emission (λ_{em}) maxima

QDs	Particle size (diameter)	λ_{abs} (nm)	λ_{em} (nm)
QD1	2.8 nm	515	530
QD2	3.5 nm	534	545
QD3	3.9 nm	560	573
QD4	4.7 nm	587	595
QD5	5.3 nm	618	626

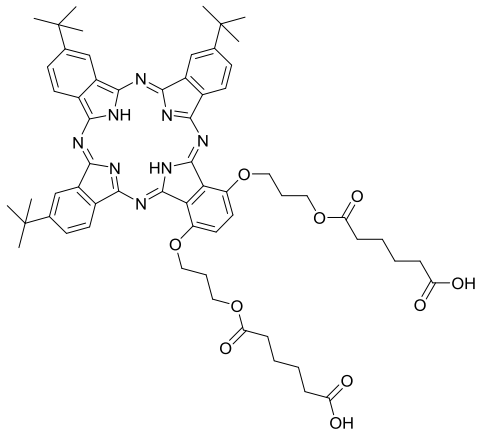

Scheme 1 The structure of the phthalocyanine used.

corrected using a correction spectrum supplied by the manufacturer.

Fluorescence decays were measured using a time-correlated single photon counting (TCSPC) system (PicoQuant GmBH). Samples were placed in a 1 cm cuvette. The excitation wavelength was 483 nm for all samples to minimize absorption by Pc when exciting the QDs. Fluorescence was measured with a microchannel plate photomultiplier tube (Hamamatsu R2809U). The time resolution of the TCSPC measurements was about 110 ps.

A pump–probe technique was used to measure absorption kinetics of the sample in the time domain from femtoseconds to nanoseconds using an instrument described elsewhere.[30] All pump−probe measurements were carried out in 2 mm cuvettes with a time resolution of roughly 200 fs.

3 Results

3.1 Compounds and electrochemical measurements

The HOMO and LUMO energy levels of Pc and the higher energy edge of the QD valence band (E_{vb}) were estimated from DPV measurements (see SI Figures S2-S7). The band gaps of the QDs were calculated from the absorption and emission steady state measurements. The conduction band energies (E_{cb}) of the QDs were calculated by adding the QD band gap energy to the VB energy. The results are summarized in Table 2.

2.1 Steady state absorption

Absorption spectra of QD-Pc hybrids were recorded at different relative concentrations of Pc and a constant QD concentration of 1 μM. At low concentration of Pc (<2 μM) the spectrum is dominated by QD absorption. At higher concentration the absorption of Pc comes into play in the wavelength range 600-750 nm, but the absorption spectrum of Pc in hybrids differs gradually with increasing Pc concentration from that in chloroform solution used as a reference. This is demonstrated in Figure 1a by the example of QD2-Pc hybrids which provide reasonably good separation of QD and Pc absorption bands (spectra of other hybrids, which show similar behavior, are provided in SI, Figures S8-S16). Once the spectrum of aggregated form of Pc stabilizes (at ratios > 1:2), the absorption scales linearly with relative Pc concentration (see SI Figure S17).The broadening of the spectrum and its shift to the blue is indicative of H-type aggregation of Pc.[31] To verify this hypothesis, the spectra of low concentration samples has to be compared with

Table 2 Valence (E_{vb}) and conduction bands (E_{cb}) energies of QDs and HOMO and LUMO energies of Pc in solution.

	E_{vb}, eV	E_{cb}, eV
QD1	-5.06	-2.68
QD2	-4.98	-2.73
QD3	-5.08	-2.93
QD4	-5	-2.94
QD5	-4.9	-2.92
Pc	-4.5	-2.8

those at higher concentrations. Since the spectra of the QDs do not change upon addition of Pc, the spectra of Pc chromophores can be obtained by subtracting QD spectrum from the spectra of the QD-Pc hybrids. These measurements were carried out in the relative Pc to QD concentration range from 0.1 to 10; to monitor the spectral change the subtracted spectra were normalized at the Pc absorption maximum, as presented in Figure 1b. At low concentrations of Pc, the Pc absorption spectrum is similar in shape to that of Pc in solution. Upon further addition of Pc, the shape of the absorption spectrum changes significantly.

The most distinct spectral feature at higher Pc concentrations is a broad absorption band building up at 630 nm, which resembles H-aggregates of Pc in solution.[31] The ratio of absorbance at 720 and 635 nm was used to quantify the aggregation process and its dependence on the Pc relative concentration is presented in Figure 2. The ratio decreases at low Pc concentration, saturates when the number of Pc molecules per QD reaches 3 and stays almost constant at higher Pc concentrations, indicating that roughly 3-4 Pc molecules form aggregates with characteristic spectral features well resolved in QD-Pc hybrids

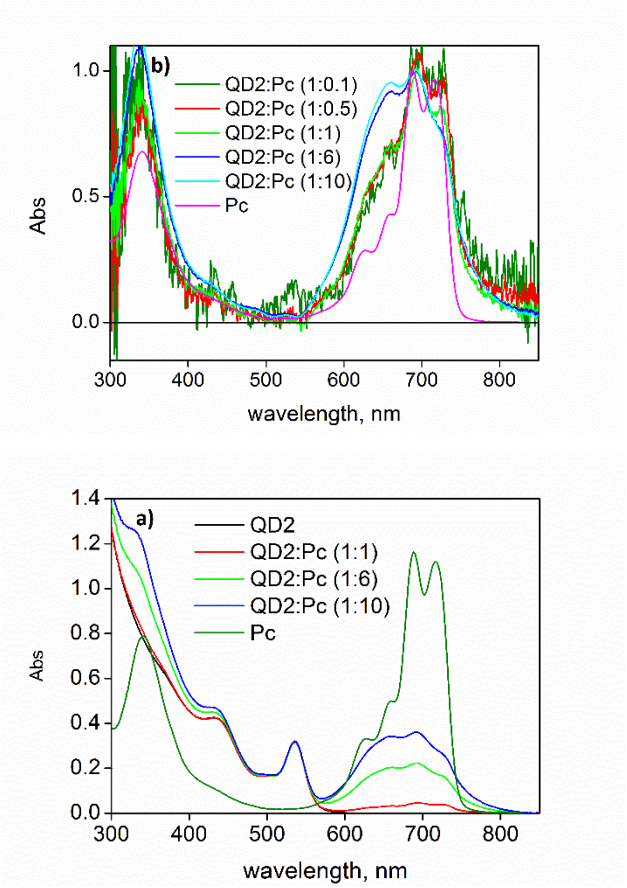

Fig. 1 (a) Absorption spectra of QD2, Pc and QD2-Pc hybrids at different concentrations of Pc in $CHCl_3$ solution. (b) Normalized absorption spectra of Pc in the QD-Pc hybrids at different relative concentrations of Pc obtained by subtracting the spectrum of QDs from that of the complex.

3.2 Emission quenching of QDs by Pc

Emission spectra of QD3-Pc hybrids with different relative concentrations of Pc are shown in Figure 3. The QD emission is quenched upon addition of Pc with the quenching efficiency reaching 90% at a QD:Pc ratio of 1:10, although the position and shape of the emission band remains the same (see SI Figures S18-21). At the same time, the emission intensity of Pc does not increase steadily with concentration, as would be expected for an energy transfer quenching mechanism.

The concentrations of QDs were estimated based on the supplier's specification corrected by comparison with the results of Jasieniak et al. linking QD band gap and molar absorption.[5]

3.3 Emission decays

TCSPC was used to determine the emission lifetimes of the pure QDs, pure Pc and QD-Pc hybrids. The results of the measurements of QD3-Pc samples are presented in Figure 4 (see SI Figures S23-26 for other QD-Pc hybrids). The samples were excited at 483 nm which excites the QD selectively, and emission was monitored at 600 nm, which allows the decay of QD excited state to be monitored. The fluorescence of Pc was measured separately by

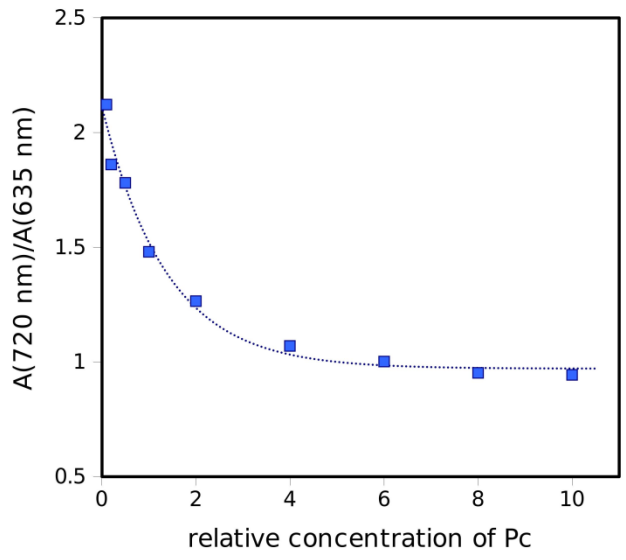

Fig. 2 Dependence of the Pc absorbance ratio at 720 and 635 nm on the relative concentration of Pc.

exciting the samples at 650 nm and monitoring the emission at 710 nm. The fluorescence decay of the Pc sample was purely mono-exponential with a lifetime of 5.43±0.03 ns. In contrast, the emission decays of QD samples are essentially multi-exponential even for pure QD samples and become more complex upon addition of Pc. This is expected, as QD-Pc hybrids are heterogeneous

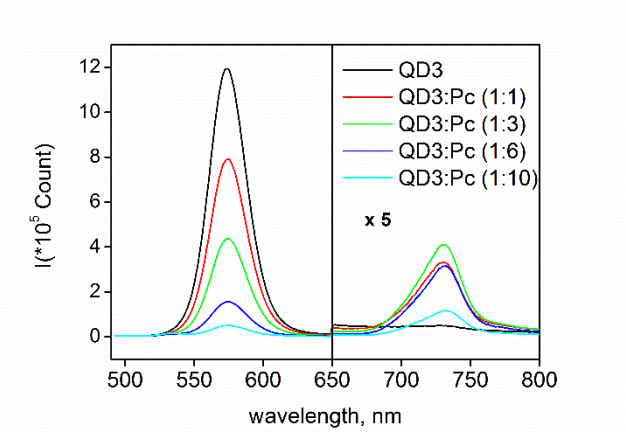

Fig. 3 Emission spectra of the QD3 and QD3-Pc hybrids at different relative Pc concentrations (indicated in the plot). The excitation wavelength is 483 nm. The longer wavelength parts of spectra (>650) are magnified five times.

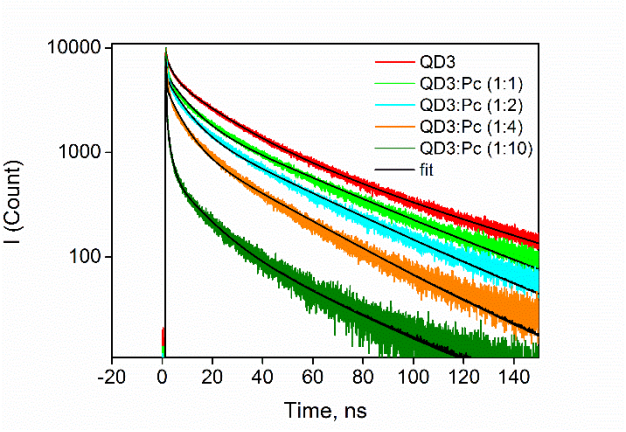

Fig. 4 Emission decays of QD3-Pc samples at 600 nm. The excitation wavelength is 483 nm. Concentration ratios are indicated in the plot. The black lines show best fits to the data.

systems. Although a multi-exponential fit was applied to the decay curves, the obtained lifetimes provide little useful information when considered alone.

A few general trends can be seen in the change of the emission decay profile as the relative concentration of Pc increases. First, the shortest lifetime decreases significantly upon adding Pc, and is at the limit of the instrument time resolution. Second, the longest lifetime remains almost constant. Third, the relative intensity of the fast decay component increases with Pc concentration. This type of behavior is in agreement with statistical formation of the hybrids and QD emission quenching through interaction with Pc.[19,21,32] The long-lived component is due to the QD population without Pc and decreases sharply as the relative concentration of Pc increases. Accordingly, the relative contribution of the fast component increases with Pc concentration and its average time constant decreases, since statistically more quenchers are attached to each QD.

3.4 Transient absorption

Selective excitation of Pc is achieved at 690 nm, since none of the QDs absorb light at this wavelength. Predominant excitation of QDs is achieved at 480 nm, since at this wavelength absorption of Pc is

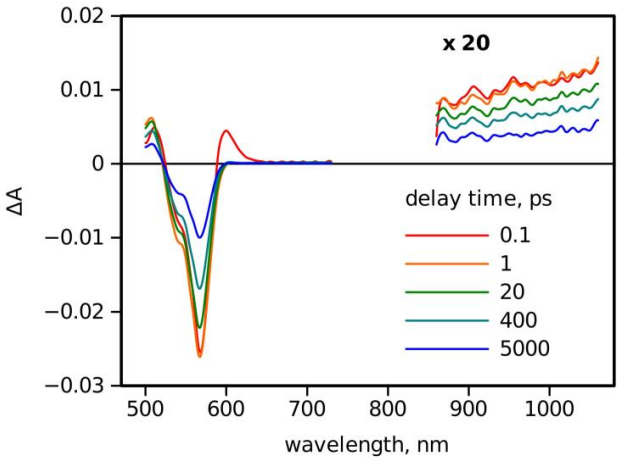

Fig. 5 Time resolved transient absorption spectra of QD3 at selected delay times indicated in the plot. The NIR part is magnified by a factor 20 for clarity.

minimal. Therefore, two excitation wavelengths 480 and 690 nm, were used for transient absorption studies. However, at 480nm, there is still some residual Pc absorption, which starts to show up at high Pc concentration. Therefore, the measurements were carried out on QD-Pc hybrid samples with a QD:Pc ratio of 1:7, where the absorbance of the Pc is less than 5% of that of QDs for all samples. A relatively high concentration of Pc was used to reduce the statistical population of free QDs and thus to make the system more homogeneous. There was no change in the absorption spectrum of the samples after the measurements, which rules out photodegradation of QDs during the experiments. Time resolved transient absorption spectra of QD3 sample are shown in Figure 5. To achieve a reasonable data fit, a five exponential model was necessary, which reflects the heterogeneity issue but does not help much in understanding the photophysics of the system. The results of the fit are presented in Figures S27-32, but essential conclusions can be made already from the time resolved spectra. The general features of the transient absorption spectra of QDs alone are a strong signal coming from the ground state absorption depletion at lowest energy absorption maximum, some spectral perturbations at shorter wavelengths, which are not of concern for this study, and a weak response in the near infrared (NIR) part of the spectrum. There is a fast decay component, 0.2-0.4 ps, which was observed in all measurements with selective excitation of QD and is much faster than the time scale of the QD-Pc interaction. This has been seen in previous studies and is attributed to the thermal relaxation of the system to the lowest energy excited state.[33,34] This component is not relevant to our study and will not be discussed further.

The spectrum of the remaining part of the transient absorption does not change, which indicates that there are no new intermediate states formed and the only observed process is the relaxation to the ground state. The fast relaxation occurs over a range of time constants from picoseconds to hundreds of picoseconds, and can be attributed to traps and defects in just over half of the QDs. The dominant part of the relaxation takes place with a time constant longer than the available delay time of the instrument, 6 ns, and can be attributed to the relaxation of defect-free QDs. The emission decay measurements discussed above give a more accurate estimate of the lifetime, which is close to 20 ns for all QDs. These results are typical for core only CdSe QDs.[33]

Transient absorption measurements of a pure Pc sample were undertaken and gave results consistent with previous studies.[35] However it should be noted that Niemi et al. have reported photophysics of the Pc monomers, whereas Pc in QD-Pc hybrids are aggregated, have rather different absorption spectra, and almost certainly have different photophysical properties. To address this issue, QD-Pc hybrids were studied with selective excitation of Pc at 690 nm. This study can also answer the question of the interaction of photoexcited Pc with QD. Figure 6 presents time resolved

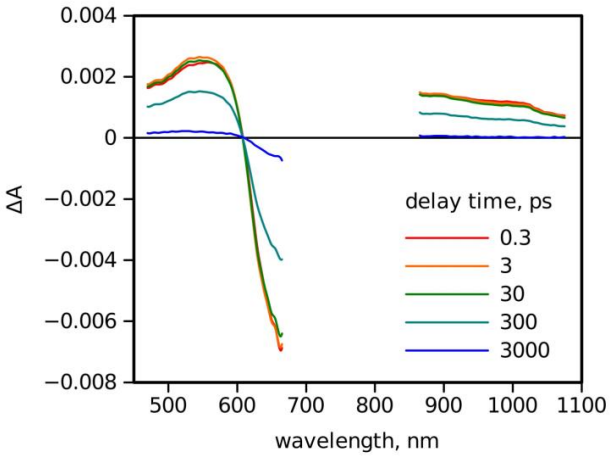

Fig. 6 Time resolved transient absorption spectra of the QD1-Pc (1:7) sample excited at 690 nm. The delay times are indicated in the plot.

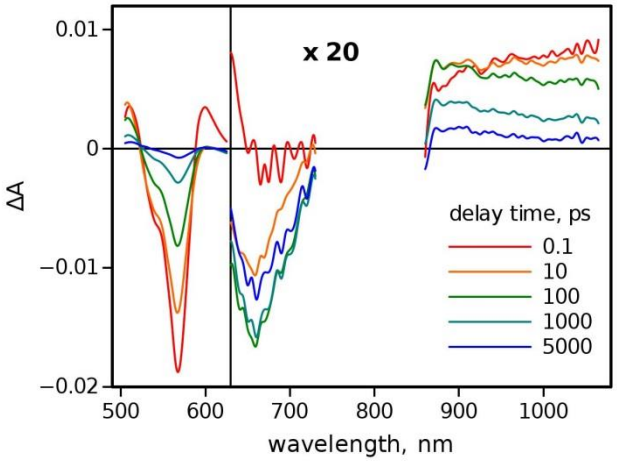

Fig. 7 Time resolved transient absorption spectra of the QD3-Pc (1:7) sample excited at 480 nm. The responses at >630 nm are magnified by a factor of 20. Delay times are indicated in the plot.

transient absorption spectra of a QD1-Pc sample excited at 690 nm as an example; the QD1 system is shown because it shows the clearest separation of ground state absorption bands. The same results were obtained for other hybrids. The first important qualitative observation is that the transient absorption response comes exclusively from Pc aggregates in this case, meaning that the photoexcited Pcs do not interact with the QDs regardless of QD size. A quantitative analysis carried out by applying global fits to the transient absorption data revealed a fast component (<1 ps) attributed to the thermal relaxation to the lowest excited state. It is not essential for our further consideration. At delay times longer than 1 ps the shape of the spectrum does not change, but the decay profile is not mono- exponential and was modeled by a bi-exponential function. The dominating (>90%) fast component had time constant 450-480 ps and the remaining part decayed with a roughly 5 ns time constant. Considering that for monomeric Pc the singlet excited state lifetime is 5 ns, the longer lifetime can be attributed to monomeric Pc molecules, but this is a minor population which has less than 10% effect on the excitation relaxation of Pc. The transient absorption response of the hybrid samples excited at 480 nm were more complex and indicated that both parts, QDs and Pc, are involved in the excitation relaxation. Figure 7 presents the transient absorption spectra at a few characteristic delay times for the QD3-Pc (1:7) sample as an example. Right after the excitation (at 0.1 ps delay time) the transient absorption spectrum is virtually identical to that of the QD3 sample alone, as can be expected since at this wavelength QDs are excited predominantly. However, already at a few ps delay time a depletion of the Pc Q-bands appears. It is clearly seen at 10 ps delay and the depletion is maximal at delay time close to 200 ps. Within this delay time the initial bleaching of the QD ground state absorption at 570 nm recovers only partially, indicating that the QD are not returning to the ground state as Pc becomes involved in excitation relaxation. There is also noticeable spectral change in the near IR region. Right after excitation the intensity of the transient absorption increases marginally toward the longer wavelengths, which correlates well with the response of QD alone. The spectrum changes shape with time, such that the stronger absorption shifts to

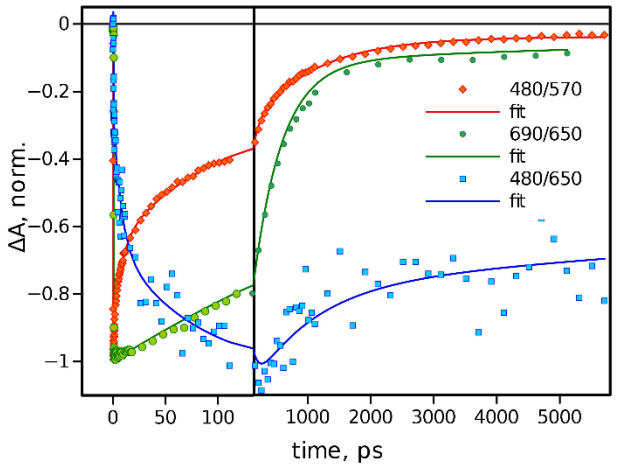

Fig. 8 Normalized transient absorption decay traces of QD3-Pc sample excited at 480 and 690 nm, and monitored at 570 and 650 nm. Two numbers in the legend indicate excitation/monitoring wavelengths. The time axis has two linear scales broken at 140 ps. Symbols are measured data and solid lines are the fits (see text for details).

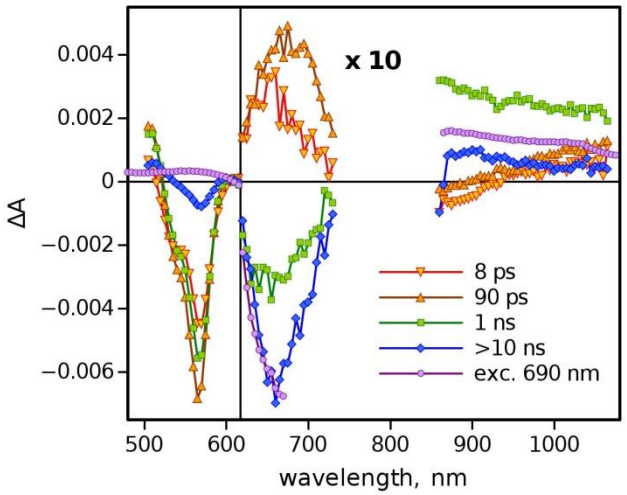

Fig. 9 Transient absorption decay component spectra of QD3-Pc (1:7) sample. Obtained with excitation at 480 nm (time constants are indicated in the plot) and recovery component of the same sample obtained with excitation at 690 nm (see text for details). The spectra at > 650 are magnified by factor of 10.

the shorter wavelength, but the total signal intensity stays practically the same. The absorption intensity in the NIR range does not change noticeably within the first 100 ps, but the bleaching of the QD band at 570 nm recovers by more than 60% within the same time interval. This is in sharp contrast to the transient absorption response recorded for the QD alone, whereby the signal decays synchronously in the visible and NIR parts of the spectrum. These results suggest that the main part of the signal in the NIR comes from Pc at a delay time of 100 ps and longer.

It is also instructive to compare transient absorption traces at two absorption maxima of QD (570 nm) and Pc (650 nm) obtained with the selective excitation of QD (at 480 nm) and Pc (at 690 nm). This comparison is presented in Figure 8 for the QD3-Pc (1:7) sample with signals normalized to -1 at maximum bleaching of 570 and 650 nm absorption bands. Three obvious conclusions can be made based on this data presentation. First, there is a good correlation between the rise of the Pc Q-band bleaching and decay of the QD absorption band at 480 nm. Second, there is no visible correlation between recoveries of QD and Pc ground state absorption at delay time longer than few hundred picoseconds. Third, there is no correlation between recoveries of the Pc Q-band bleaching at two different excitation wavelengths, 480 and 690 nm.

In order to obtain quantitative information on the photoreaction in QD-Pc hybrids a global multi-exponential fit was applied, and decay components were classified as contributing to the depletion of the Pc Q-band and to recovery of the band. An example of the fit results for QD3-Pc sample is shown in Figure 9, which presents four decay component spectra; two have positive intensity around 650 nm and are attributed to delayed depletion of the Q-band (time constants 8 and 90 ps), while the other two have negative intensity at 650 nm and thus present recovery of the Pc ground state absorption (time constants are 1 and >10 ns). In addition, a recovery spectrum of the same sample excited at 690 nm is shown. The time constants of the delayed depletion of the Q-band with weights taken as

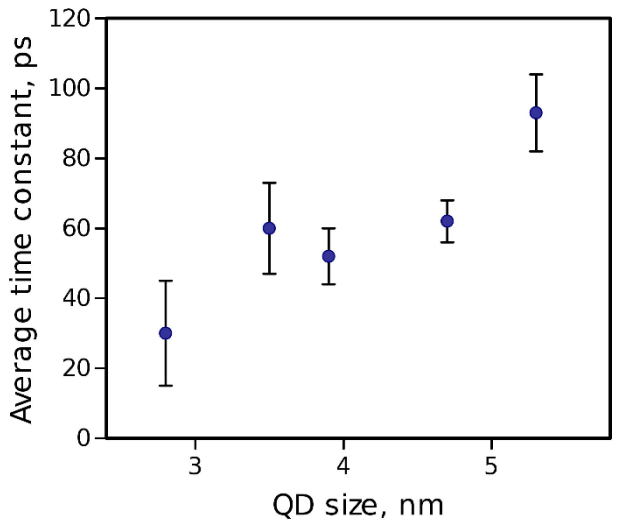

Fig. 10 The dependence of the average time constant of delayed depletion of the Pc Q band on the size of QD in QD-Pc hybrids.

corresponding spectrum intensities at 650 nm were used to calculate the average time constants for this process and the results of the calculations are presented in Figure 10 as a function of the QD Size.

4 Discussion

Addition of Pc to a QD suspension results in the gradual decrease in QD emission intensity as well as in the shortening of the emission lifetime. Apparently, Pc quenches the QD excited state. Two mechanisms could be responsible for the quenching, an energy transfer and a charge transfer. The former should lead to the appearance of a Pc singlet excited state after the relaxation of a QD excited state and the latter to the formation of charged species, presumably QD^- and Pc^+. In the case of energy transfer, the QD returns to the ground state after transferring energy to Pc, meaning that the expected outcome is a complete recovery of the QD bleaching at the end of the process. This is not the case in our system, as at the delay time of the maximum signal at the Pc Q-band, around 200 ps, the QD response at 570 nm recovers by only 65% (Figure 8). This is the first experimental observation to question energy transfer as the mechanism of the QD excited state quenching. A charge transfer mechanism does not return the QD to the ground state and does not contradict partial recovery of the QD ground state absorption.

The energy transfer from the QD should result in formation of the Pc singlet excited state. The spectrum of latter was determined experimentally from the same sample by switching excitation to 690 nm, and the corresponding spectrum is shown in Figure 9 (marked as “exc. 690 nm”). There is no match between this spectrum and long-lived decay spectra obtained with excitation at 480 nm. This is the second experimental observation in contradiction to the energy transfer hypothesis. In addition, once the Pc singlet excited state is formed, it must decay independently of the mechanism which led to its formation, but decay traces at 650 nm obtained with different excitations are different (Figure 8, “480/650” and “690/650” traces). This is the third reason to rule out energy transfer as the main relaxation mechanism.

The fourth argument to reject energy transfer comes from the average time constant dependence on the QD size presented in Figure 10. The two most important factors affecting the time constant of the energy transfer are the spectral overlap integral and the distance between the Pc chromophore and the QD. The overlap integral measures the overlap between the emission spectrum of the donor, QD, and absorption spectrum of the acceptor, Pc, and can be estimated from the emission spectra of the QDs and absorption spectra of Pc aggregates in QD-Pc hybrids. The overlap integral is largest for QD5-Pc and relative to that it decreases to 36%, 20%, 2% and 3% for QD4-Pc, QD3-Pc, QD2-Pc and QD1-Pc, respectively (see SI Figure S22). The overlap integral factor predicts roughly 30 times faster energy transfer in QD5-Pc compared to that

in QD2-Pc hybrids, which is in sharp contradiction with dependence shown in Figure 10. For the distance estimation, we assume that the distance between the QD surface and the Pc chromophore is a roughly the same for all QDs, 1 nm, based on the length of the linker. Then, taking point dipole-dipole energy transfer approximation and placing the dipoles in the center of QD and Pc gives center-to-center distances of 2.4 and 3.7 nm for QD1-Pc and QD5-Pc hybrids, respectively. Since Förster energy transfer follows a power six dependence on center to center distances R,[36] it would predict a ratio of $(R_5/R_1)^6 = (3.7/2.4)^6 = 13$, for the energy transfer in QD5-Pc (R_5) compared to that in QD1-Pc (R_1), which does not outweigh the overlap integral factor. Thus the observed dependence does not agree with a Förster energy transfer quenching mechanism.

The second alternative mechanism to explain the excited state quenching is charge transfer. Charge separated states are usually identified by characteristic anion and cation bands. It has been reported that the spectrum of positively charged CdSe QD is virtually identical to that of the ground state.[19,22] It has been shown that negatively charged CdSe QDs have reduced absorption at lowest energy absorption band, [37] which means that partial recovery of the QD ground state absorption is consistent with charge separation, namely formation of the QD^--Pc^+ state after QD excited state relaxation.

Pc cations are expected to have a band around 850-900 nm, [35] although this band was observed for non-aggregated states of Pc derivatives; in aggregated states the cation spectra may differ gradually. Nevertheless, the spectral changes in the NIR region show that a state with an enhanced absorption close to 850 nm is formed simultaneously with growing depletion of the Q-band absorption (Figure 7). This band cannot be attributed to the Pc singlet excited state, which has a much flatter absorption in the NIR range (Figure 6). The second reason to attribute it to a Pc cation is that the relaxation time profile of this state does not agree with that of the singlet excited state as was discussed above.

The charge transfer model agrees well with the dependence shown in Figure 10. The energy of the excited state increases as the QD size decreases, resulting in a higher driving force for the charge separation reaction. This predicts a faster charge separation for smaller QDs in the Marcus normal region.[38]

The decay component with a 1 ns time constant has the most distinct NIR feature with a broad absorption band close to 850 nm (Figure 9). It can be attributed to the charge recombination. It also shows an almost complete recovery of the QD ground state (time resolved spectrum at 5000 ps delay in Figure 7) as is expected for the charge recombination. However, there is a much longer lived bleaching of the Pc Q-band, which goes beyond the measurements time scale of the instrument (6.5 ns) and is indicated as a component with lifetime >10 ns in Figure 9. This component has a relatively weak and flat absorption in the NIR part of the spectrum and it is tentatively attributed to the Pc triplet excited state, though there is no plausible proof of the nature of this state.

Direct excitation of Pc in QD-Pc hybrids does not result in charge separation or in any other detectable interaction between QD and Pc. This indicates that the energy of the charge separated state, QD^--Pc^+, is higher than that of the singlet excited state of Pc, Pc^S. This is in contrast to the DPV results, which indicated that the conduction bands of the QDs lie lower than the LUMO of Pc. The DPV results were obtained for QDs alone and Pc alone, and can only be seen as rough estimates for the energies in QD-Pc hybrids. Energies in hybrids may differ both because of Coulombic interactions in the charge separated state and because of

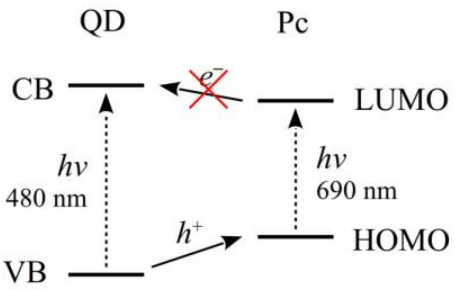

Fig. 11 Energy diagram for QD-Pc hybrids.

aggregation of Pc. The results of this investigation do not provide any evidence of electron transfer from the LUMO of Pc to the CB of QDs. In particular, there is no visible interaction when Pc is excited directly. Apparently the excited state energy of aggregated Pc is not sufficiently high for the electron transfer to take place from the Pc LUMO to the QD conduction band. However, excitation of QD leads to the formation of the charge separated state identified as QD^{-}-Pc^{+}. It cannot be electron transfer from the QD conduction band, since this would lead to formation of a Pc anion and a QD cation. Therefore, it must be hole transfer from the QD VB to the HOMO of Pc, as explained in the energy diagram presented in Figure 11. The hole transfer was previously proposed as mechanism of photoinduced charge separation in QD hybrids with bithiophene,[26] phenothiazine[39] and dopamine.[40]

Assuming that the Pc LUMO energy is just on the level of the CB of the largest QD (2.92 eV according to Table 2) and taking band gap energies from the optical properties of QD and Pc (1.98 and 1.75 eV, respectively), one obtains a driving force for the hole transfer from the VB to the HOMO of 0.23 eV. This value is most probably smaller than the reorganization energy associated with the charge separation reaction, which was reported to be >0.3 eV for phthalocyanine based donor-acceptor systems.[41] Therefore, the charge transfer process is expected to be in the normal Marcus regime, as discussed above. It is interesting to note that if the charge separation took place from the Pc excited state, and thus were an electron transfer from the Pc LUMO to the QD CB, an opposite dependence on QD size would be expected, since for smaller QDs the driving force would be smaller and electron transfer slower.

5 Conclusions

A consideration of thermodynamics is typically the key to designing systems with desired photoinduced charge transfer functionality. However, direct and accurate experimental evaluation of energy states is complicated when markedly different components, such as semiconductor QDs and organic dyes, are used to design such donor-acceptor systems. Although the electrochemical measurements of CdSe QDs and Pc used in this study suggested that an electron transfer from the excited Pc to QD is thermodynamically possible, experimental results show clearly that the reaction does not take place within the lifetime of the Pc excited state. Nevertheless, the charge separation takes place in this QD-Pc hybrids but it requires photo-excitation of the QD, and is a hole transfer from the photoexcited the QD to the non-excited Pc.

Acknowledgments

The Academy of Finland (grant 263486) and TUT's graduate school are acknowledged for funding.

Notes and references

1 B. Guzelturk, P. L. H. Martinez, Q. Zhang, Q. Xiong, H. Sun, X. W. Sun, A. O. Govorov and H. V. Demir, *Laser Photon. Rev.*, 2014, **8**, 73–93.

2 K. S. Leck, Y. Divayana, D. Zhao, X. Yang, A. P. Abiyasa, E. Mutlugun, Y. Gao, S. Liu, S. T. Tan, X. W. Sun and H. V. Demir, *ACS Appl. Mater. Interfaces*, 2013, **5**, 6535–6540.

3 M. Ye, X. Wen, M. Wang, J. Iocozzia, N. Zhang, C. Lin and Z.

Lin, *Mater. Today*, 2014, **18**, 155–162.

4 J. Jasieniak, M. Califano and S. E. Watkins, *ACS Nano*, 2011, **5**, 5888–5902.

5 J. Jasieniak, L. Smith, J. Van Embden, P. Mulvaney and M. Califano, *J. Phys. Chem. C*, 2009, **113**, 19468–19474.

6 E. Galoppini, *Coord. Chem. Rev.*, 2004, **248**, 1283–1297.

7 R. Naaman, *Phys. Chem. Chem. Phys.*, 2011, **13**, 13153–13161.

8 J. E. Greene, *Appl. Phys. Rev.*, 2015, **2**, 011101.

9 B. Ketterer, A. V Kuhlmann, J. Houel and J. R. Morante, *Nat. Mater.*, 2013, **12**, 439–444.

10 Z. Xu, C. R. Hine, M. M. Maye, Q. Meng and M. Cotlet, *ACS Nano*, 2012, **6**, 4984–4992.

11 H. Song, M. A. Reed and T. Lee, *Adv. Mater.*, 2011, **23**, 1583–1608.

12 S.-J. Kim, M. Naruse, M. Aono, M. Ohtsu and M. Hara, *Sci. Rep.*, 2013, **3**, 2370.

13 A. Boulesbaa, Z. Huang, D. Wu and T. Lian, *J. Phys. Chem. C*, 2010, **114**, 962–969.

14 A. Pal, S. Srivastava, P. Saini, S. Raina, P. P. Ingole, R. Gupta and S. Sapra, *J. Phys. Chem. C*, 2015, **119**, 22690–22699.

15 M. H. Stewart, A. L. Huston, A. M. Scott, E. Oh, W. R. Algar, J. R. Deschamps, K. Susumu, V. Jain, D. E. Prasuhn, J. Blanco-canosa, P. E. Dawson and I. L. Medintz, *ACS Nano*, 2013, **7**, 9489–9505.

16 E. S. Shibu, A. Sonoda, Z. Tao, Q. Feng, A. Furube, S. Masuo, L. Wang, N. Tamai, M. Ishikawa and V. Biju, *ACS Nano*, 2012, **6**, 1601–1608.

17 J. H. Bang and P. V. Kamat, *ACS Nano*, 2011, **5**, 9421–9427.

18 H. Choi, R. Nicolaescu, S. Paek, J. Ko and P. V. Kamat, *ACS Nano*, 2011, **5**, 9238–9245.

19 K. Virkki, S. Demir, H. Lemmetyinen and N. V Tkachenko, *J. Phys. Chem. C*, 2015, **119**, 17561–17572.

20 Z. Xu and M. Cotlet, *Angew. Chem. Int. Ed.*, 2011, **50**, 6079–6083.

21 N. Song, H. Zhu, S. Jin, W. Zhan and T. Lian, *ACS Nano*, 2011, **5**, 613–621.

22 A. J. Morris-Cohen, M. T. Frederick, L. C. Cass and E. A. Weiss, *J. Am. Chem. Soc.*, 2011, **133**, 10146–10154.

23 V. V. Chaban, V. V. Prezhdo and O. V. Prezhdo, *J. Phys. Chem. Lett.*, 2013, **4**, 1–6.

24 A. L. Kaledin, T. Lian, C. L. Hill and D. G. Musaev, *J. Phys. Chem. B*, 2015, **119**, 7651–7658.

25 S. Jin, M. Tagliazucchi, H. J. Son, R. D. Harris, K. O. Aruda, D. J. Weinberg, A. B. Nepomnyashchii, O. K. Farha, J. T. Hupp and E. A. Weiss, *J. Phys. Chem. C*, 2015, **119**, 5195–5202.

26 A. Iagatti, R. Flamini, M. Nocchetti and L. Latterini, *J. Phys. Chem. C*, 2013, **117**, 23996–24002.

27 H. Imahori, T. Umeyama and S. Ito, *Acc. Chem. Res.*, 2009, **42**, 1809–1818.

28 G. Bottari, O. Trukhina, M. Ince and T. Torres, *Coord. Chem. Rev.*, 2012, **256**, 2453–2477.

29 A. P. Brown and F. C. Anson, *Anal. Chem.*, 1977, **49**, 1589–1595.

30 B. Pelado, F. Abou-Chahine, J. Calbo, R. Caballero, P. de la Cruz, J. M. Junquera-Hernández, E. Ortí, N. V. Tkachenko and F. Langa, *Chem. - A Eur. J.*, 2015, **21**, 5814–5825.

31 S. Kakade, R. Ghosh and D. K. Palit, *J. Phys. Chem. C*, 2012, **116**, 15155–15166.

32 J. Huang, Z. Huang, S. Jin and T. Lian, *J. Phys. Chem. C*, 2008, **112**, 19734–19738.

33 P. Kambhampati, *Chem. Phys.*, 2015, **446**, 92–107.

34 V. I. Klimov, *Phys. chem. B*, 2000, **104**, 6112–6123.

35 M. Niemi, N. V. Tkachenko, A. Efimov, H. Lehtivuori, K. Ohkubo, S. Fukuzumi and H. Lemmetyinen, *J. Phys. Chem. A*, 2008, **112**, 6884–6892.

36 R. M. Clegg, *Curr. Opin. Biotechnol.*, 1995, **6**, 103–10.

37 J. D. Rinehart, A. M. Schimpf, A. L. Weaver, A. W. Cohn and D. R. Gamelin, *J. Am. Chem. Soc.*, 2013, **135**, 18782–18785.

38 R. A. Marcus, *Angew. Chemie Int. Ed.*, 1993, **32**, 1111–1121.

39 S. Lian, D. J. Weinberg, R. D. Harris, M. S. Kodaimati and E. A. Weiss, *ACS Nano*, 2016, **10**, 6372−6382.

40 X. Ji, N. S. Makarov, W. Wang, G. Palui, I. Robel and H. Mattoussi, *J. Phys. Chem. C*, 2015, **119**, 3388−3399.

41 F. Ito, Y. Ishibashi, S. R. Khan, H. Miyasaka and Y. Kobuke, *J. Phys. Chem. A*, 2006, **110**, 12734–12742.